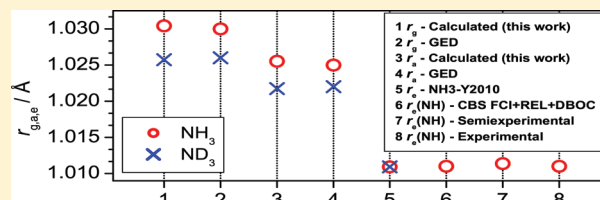


Temperature-Dependent, Effective Structures of the $^{14}\text{NH}_3$ and $^{14}\text{ND}_3$ Molecules

István Szabó, Csaba Fábri, Gábor Czakó, Edit Mátyus, and Attila G. Császár*

Laboratory of Molecular Structure and Dynamics, Institute of Chemistry, Eötvös University, H-1518 Budapest 112, P.O. Box 32, Hungary

ABSTRACT: Measurements result in effective, usually temperature-dependent structural parameters of molecules, and never directly in equilibrium structures, which are theoretical constructs. A recent high-accuracy semiglobal potential energy surface of the electronic ground state of the ammonia molecule, called NH3-Y2010 (*J. Mol. Spectrosc.* **2011**, 268, 123), which exhibits mass-independent equilibrium NH bond length and a HNH bond angle of 1.0109 Å and 106.75°, respectively, is employed together with the variational nuclear motion code GENIUSH (*J. Chem. Phys.* **2009**, 130, 134112; **2011**, 134, 074105) to determine directly measurable, effective structural parameters of the $^{14}\text{NH}_3$ and $^{14}\text{ND}_3$ molecules. The effective r_g - and r_a -type NH(ND) distances determined at 300 K are 1.0307(1.0254) and 1.0256(1.0217) Å, respectively, with an estimated accuracy of 2×10^{-4} Å. The effective θ_g HNH and DND bond angles at 300 K are 106.91° and 106.85°, respectively. The root-mean-square amplitudes of vibration, l_g , for the NH(ND) distances at 300 K are 0.073(0.062) Å. These structural parameters confirm the less accurate results of a room-temperature gas-electron-diffraction study (*J. Chem. Phys.* **1968**, 49, 2488, all data in Å): $r_g(\text{NH}) = 1.030(2)$, $l_g(\text{NH}) = 0.073(2)$, $r_g(\text{ND}) = 1.027(3)$, and $l_g(\text{ND}) = 0.061(2)$. The computed difference in the $r_{g,T}(\text{NH})$ bond lengths of the two spin isomers (ortho and para forms) of $^{14}\text{NH}_3$ is 3×10^{-5} Å at 0 K, the difference diminishes at temperatures of about 30–50 K.



■ INTRODUCTION

The Born–Oppenheimer (BO) approximation^{1–3} introduces the separation of nuclear and electronic motions of molecules and leads to the concepts of electronic potential energy (hyper)surfaces (PES)^{4–6} and equilibrium structures.⁷ The latter correspond to molecular configurations at local minima of PESs.^{7–18} Despite being an extremely important chemical concept, equilibrium structures of molecules cannot be determined experimentally in a direct way. Experiments can only provide temperature-dependent, effective structures and structural parameters. It is well-known that there are intrinsic and sizable differences between the equilibrium (r_e) and the experimentally derived (r_a , r_w , r_c , r_g , r_m , r_s , r_z , etc.) structural parameters.^{7,12–14,19} These differences and even differences among the different averaged parameters are of similar magnitude as, for example, the geometry effect of substitutions in a series of molecules. Furthermore, experimental, effective structures may deviate from the equilibrium ones even in a qualitative way.¹⁸

The present investigation of the effective structures of ammonia is similar to an earlier study on water isotopologues¹⁷ performed employing fourth-age²⁰ quantum chemical methods. Both studies aim to investigate how the direct quantum chemical route allows us to move from “static”, purely theoretical equilibrium structures to temperature-dependent, effective structural parameters corresponding to measurable ones.

Ammonia was chosen as the model compound of this investigation for several reasons. (1) It is a simple, stable four-atomic chemical species, it is one of the principal deposits of nitrogen in molecules, and it provides one of the most accurate “molecular thermometers” for the interstellar medium.²¹ (2) Because ammonia contains “only” four nuclei and 10 electrons,

it is among the few polyatomic molecules for which highly sophisticated quantum chemical (electronic and nuclear motion) computations have become feasible during the past decade or so. Therefore, accurate PESs, resulting in accurate estimates of equilibrium structures have been derived for ammonia.^{22–34} (3) The quantum chemical model of the ammonia molecule is characterized by a large-amplitude motion called inversion exhibiting a symmetric double-well potential.^{35–39} The height of the effective barrier is $2021 \pm 20 \text{ cm}^{-1}$ when relativistic effects ($+20 \text{ cm}^{-1}$), Born–Oppenheimer diagonal corrections (-10 cm^{-1}), and zero-point vibrations ($+244 \text{ cm}^{-1}$) are considered.^{36,37,40,41} Treating the inversion motion is challenging for perturbative approaches and calls for variational nuclear motion treatments.^{42–46} (4) The structure of ammonia has been studied experimentally in considerable detail both by spectroscopic methods^{47–49} and by gas electron diffraction (GED).^{50–53} Among many other results, GED investigations yielded effective structural parameters for two isotopologues of ammonia, $^{14}\text{NH}_3$ and $^{14}\text{ND}_3$, at room temperature.⁵² Note also that the equilibrium NH bond length of several molecules was analyzed by Demaison et al.⁵⁴ (5) The parent isotopologue of ammonia, $^{14}\text{NH}_3$, exists in two nuclear-spin isomer forms (Table 2, vide infra), ortho (proton quartet) and para (proton doublet), which correspond to different values of the total nuclear spin (I) of the three H atoms. Symmetry requirements⁵⁵ ensure that the value of K for $o\text{-NH}_3$ is a multiple of 3 ($K = 3n$, $n = 0, 1, 2, \dots$), whereas $p\text{-NH}_3$ has values of $K = 3n \pm 1$ (K is the usual

Received: December 7, 2011

Revised: April 3, 2012

Published: April 3, 2012

molecule-fixed projection quantum number of a rotating symmetric top).

THEORETICAL BACKGROUND

PES. In this study a sophisticated, “spectroscopic” PES of ammonia, determined by Yurchenko et al.,³⁴ is employed for the nuclear motion computations. This PES, called NH3-Y2010, is capable to reproduce the experimentally known term values with a root-mean-square deviation of 0.2 cm⁻¹.³⁴ It must be noted that the kinetic energy operator (KEO) employed in the nuclear motion computations by Yurchenko et al.³⁴ to fit the PES contains approximations and thus nuclear motion computations with a complete KEO, like the one employed in this study, may lead to larger discrepancies with respect to experiment.⁴⁶

Equilibrium Structural Parameters. The direct route to the computation of accurate converged Born–Oppenheimer equilibrium structures, r_e^{BO} , employs systematically improved levels of electronic structure theory.⁷ This is due to the fact that for polyelectronic systems none of the limits of ab initio electronic structure theory can be reached without some sort of extrapolation and approximation.^{6,36,56} Furthermore, relativistic (REL)^{57–59} and diagonal Born–Oppenheimer (DBOC)⁶⁰ corrections must also be considered to arrive at the limits of electronic structure theory. Rajamäki et al.³⁸ provided the following estimates for the “small corrections”³⁶ on the equilibrium structural parameters of ¹⁴NH₃: $\Delta r(\text{REL}) = 0.00000 \text{ \AA}$, $\Delta\theta(\text{REL}) = -0.05^\circ$, $\Delta r(\text{DBOC}) = 0.00002 \text{ \AA}$, and $\Delta\theta(\text{DBOC}) = +0.03^\circ$, which need to be added to the nonrelativistic BO values. These values mean that both relativistic and post-BO effects on r_e^{BO} are almost negligible for this light molecule. The best estimated r_e^{ad} and θ_e^{ad} values of ref 38 are 1.0110 Å and 106.75°, respectively. These values are in nearly perfect agreement with the structural parameters of the NH3-Y2010 PES. The mass-independent (Born–Oppenheimer) equilibrium geometry on this PES of ammonia is as follows: $r_e^{\text{BO}} = 1.0109 \text{ \AA}$ and $\theta_e^{\text{BO}} = 106.75^\circ$. Note that a summary of the evolution of the estimates of the equilibrium structure of ¹⁴NH₃ is given in Table 1 of ref 54.

Nuclear Motion Computations. The full-dimensional variational rovibrational computations of this study and the determination of expectation values of the structural parameters have been performed with the in-house GENIUSH package (GENIUSH stands for general nuclear-motion code with numerical, internal-coordinate, user-specified Hamiltonians).^{45,46} The GENIUSH code employs numerically constructed complete kinetic energy operators and is able to compute eigenpairs of the (ro)-vibrational Hamiltonian corresponding to arbitrary body-fixed frames and internal coordinates defined by the user, in either full or reduced vibrational dimensionality. The matrices corresponding to the Hamiltonian are constructed using a discrete variable representation (DVR) on a direct-product grid.^{61,62} The required eigenvalues and eigenvectors of the resulting sparse Hamiltonian are provided by an iterative Lanczos⁶³ eigensolver.

In the present computations the *xyy* (scattering) frame is employed, the primitive internal coordinates are given in Table 1. A dummy atom, Y, is introduced to define the inversion coordinate, α . Nuclear masses, in u, employed in the variational rovibrational computations are $m(\text{H}) = 1.007825$, $m(\text{D}) = 2.014102$, and $m(^{14}\text{N}) = 14.003074$.

The number of optimized grid points along the actual internal coordinates ($r_1, \alpha, r_2, \beta_1, r_3, \beta_2$) (Table 1) was (10, 25, 10, 10, 10, 10). This resulted in converged wave functions and eigenvalues precise to at least 0.01 cm⁻¹ (at least an order of magnitude more precise for the lowest rovibrational states). A total of 150 pure

Table 1. Z-Matrix Representation of the Internal Coordinates of NX₃ (X = H or D)^a

N						
Y	N	1.0				
X ₁	N	r_1	Y	α		
X ₂	N	r_2	Y	α	X ₁	β_1
X ₃	N	r_3	Y	α	X ₁	$-\beta_2$

^aY is a dummy atom, introduced to define the inversion coordinate, α .

vibrational ($J = 0$) states were computed for ¹⁴NH₃ and ¹⁴ND₃, covering the energy ranges 0–6603.6 and 0–4849.7 cm⁻¹, respectively (relative to the respective zero-point vibrational energies (ZPVE)). The computed ZPVEs were 7430.28 and 5452.25 cm⁻¹ for ¹⁴NH₃ and ¹⁴ND₃, respectively. For both isotopologues and for each nonzero J value, no more than 60 rovibrational states were computed up to $J = 10$.

Expectation Value Computations. After obtaining the rovibrational wave function $|\Psi\rangle$, determination of the expectation value of an arbitrary function f involves the integral $\langle\Psi_{\mathbf{v},J,K}|f|\Psi_{\mathbf{v},J,K}\rangle$, where \mathbf{v} and J, K stand for vibrational and rotational labels, respectively. Here \mathbf{v} is a collective index of normal-mode “quantum” numbers representing the six internal degrees of freedom, \mathbf{q} , of the molecule, J , in the absence of an external field, is a “good” quantum number corresponding to the overall rotation of the molecule, and K is the usual molecule-fixed projection quantum number characterizing overall rotations of a symmetric top. Expectation values of a function $f(\mathbf{q})$ in a DVR are given by the sum

$$\langle f(\mathbf{q}) \rangle_{\mathbf{v},J,K} = \sum_{i=1}^N \sum_{l=1}^{2J+1} (C_{il}^{\mathbf{v},J,K})^2 f(\mathbf{q}_i) \quad (1)$$

where matrix $C^{\mathbf{v},J,K}$ contains the eigenvectors of the nuclear Hamiltonian, \mathbf{H}^{DVR} , represented in a DVR, and the N grid points in the multidimensional space are \mathbf{q}_i .^{64,65} (We note that in GENIUSH the grid points are not coupled to the rotational functions.) If a macroscopic sample of ammonia is in thermal equilibrium, we can rely on the Boltzmann distribution for the calculation of effective temperature-dependent structural parameters.⁷

Two temperature-dependent distance types are considered here, $r_{g,T}$ (g stands for “center of gravity”) and $r_{a,T}$, denoting the “mean” and “inverse” thermal average values of a given internuclear distance at temperature T . They are evaluated in terms of averaged molecular quantities as follows:

$$r_{g,T} = \frac{\sum_i g_i \langle r \rangle_i e^{-(E_i - E_0)/k_B T}}{\sum_i g_i e^{-(E_i - E_0)/k_B T}} \quad (2)$$

and

$$r_{a,T} = \frac{\sum_i g_i e^{-(E_i - E_0)/k_B T}}{\sum_i g_i \langle r^{-1} \rangle_i e^{-(E_i - E_0)/k_B T}} \quad (3)$$

In the above expressions E_0 is the zero-point energy, E_i is the rovibrational energy determined in the nuclear motion computations, k_B is Boltzmann’s constant, and the averaging uses the wave functions determined in the variational nuclear motion computations. The degeneracy factor g_i of the i th rovibrational state is defined as $g_i = g_i^r g_i^K g_i^{\text{ns}}$, where, for all symmetric top molecules, $g_i^r = 2J_i + 1$ and $g_i^K = 1$ for $K_i = 0$ and 2 for all other K_i values. The nuclear spin factors g_i^{ns} are defined as $(2I_X + 1)(2I_N + 1)$, whereby I_N and I_X are the nuclear spin angular momentum quantum

Table 2. Spin Statistical Weights of the Rovibronic States of $^{14}\text{NH}_3$ and $^{14}\text{ND}_3$ Based on the $D_{3h}(\text{M})$ Molecular Symmetry (MS) Group^a

species	Γ_{rve}	stat weight	species	Γ_{rve}	stat weight
$^{14}\text{NH}_3$	A'_1	0	$^{14}\text{ND}_3$	A'_1	10
	A'_2	12		A'_2	1
	E'	6		E'	8
	A''_1	0		A''_1	10
	A''_2	12		A''_2	1
	E''	6		E''	8

^aFor $^{14}\text{NH}_3$, levels of species A'_2 and A''_2 are called ortho and levels of species E' and E'' are called para. For $^{14}\text{NH}_3$, levels of species A'_1 and A''_1 are so-called “missing” levels.

Table 3. Equilibrium Geometry Parameters of Ammonia from ab Initio Electronic Structure Computations^a

level of theory inclusive of “small” corrections	r_e	θ_e	ref
NH3-Y2010	1.01093	106.75	34
CBS FCI+REL+DBOC ^b	1.01101	106.75	25, 38
“refined” ^c	1.01067	106.75	30
CCSD(T)/cc-pV ∞ Z ^d	1.01110	106.80	54
semiexperimental ^e	1.01139(60)	107.17(18)	68
experimental ^f	1.011(3)	106.67(20)	52

^aExperimental and semi-experimental geometries are also included for comparison. Equilibrium NH bond length (r_e) in Å, equilibrium HNH bond angle (θ_e) in degrees. ^bAdiabatic equilibrium structure; CBS = complete basis set, FCI = full CI, REL = relativistic corrections, and DBOC = diagonal Born–Oppenheimer correction. ^cSee Table 2 and section IIIA of ref 30 for detailed explanation; the PES is basically CBS FCI + REL + DBOC. ^dResults obtained by correlation of all electrons and by using diffuse functions on the N atom. ^eStructural parameters obtained from least-squares fits using experimental rotational constants and CCSD(T)/cc-pVQZ vibration–rotation interaction constants.⁶⁸ ^fEquilibrium structural parameters derived from GED results.⁵²

numbers corresponding to ^{14}N and the three $X = \text{H}$ or D nuclei, respectively. The spin statistical factors are given in Table 2 for both $^{14}\text{NH}_3$ and $^{14}\text{ND}_3$.

According to refs 66 and 67, rotational contribution to structural parameters, δr_{rot} , can be taken into account as

$$\delta r_{\text{rot}} = \sigma T \quad (4)$$

This expression gives a linear temperature dependence and the parameter σ is obtained in this work by fitting to computed Boltzmann-averaged rovibrational expectation value data. Equation 4 is then used for extrapolating the rotational contribution to elevated temperatures. This approximation was also applied in this study for averaging angles.

Another structural parameter, which characterizes traditional structural GED experiments, is the temperature-dependent root-mean-square amplitude of vibration, $l_{g,T}$, defined as⁷

$$l_{g,T} = (\langle r^2 \rangle_T - \langle r \rangle_T^2)^{1/2} \quad (5)$$

Nuclear Spin Statistics. A valid basis function for expressing the complete internal motion wave function results from the combination of a rovibronic (rve) state having symmetry Γ_{rve} and a nuclear spin state, having symmetry Γ_{ns} , whereby the direct product of the two symmetries is an allowed symmetry of the complete internal motion wave function, ψ_{int} .⁵⁵ In other words, the allowed states fulfill the $\Gamma_{\text{rve}} \otimes \Gamma_{\text{ns}} \supset \Gamma_{\text{int}}$ relation.

The existence of nuclear spin states which do not have the allowed symmetry for combination with a particular rovibronic state introduces the concept of “missing” levels. Such rovibronic levels correspond to eigenvalues of the rovibronic Hamiltonian, but no transitions will originate from or end on them because of the above symmetry restriction. In the case of $^{14}\text{NH}_3$, as can be seen in Table 2, the A'_1 and A''_1 (ro)vibrational states are not allowed due to their zero nuclear spin statistical weight factors. There are no missing levels for $^{14}\text{ND}_3$.

Table 4. $J = 1$ and 2 Term Values (J, K, ν_{inv}), in cm^{-1} , for the Lowest Four Vibrational States of $^{14}\text{NH}_3$ and $^{14}\text{ND}_3$ ^a

NH_3						ND_3					
J	K	ν_{inv}	SL	exp ^{b,c}	GENIUSH	J	K	ν_{inv}	SL	exp ^{d,e}	GENIUSH
1	1	0	E''	16.173	16.173	1	1	0	E''	8.267	8.277
1	1	1	E'	16.963	16.962	1	1	1	E'		8.331
1	0	0	A'_2	19.889	19.890	1	0	0	A'_2	10.285	10.287
2	2	0	E'	44.796	44.797	2	2	0	E'	22.785	22.821
2	2	1	E''	45.587	45.587	2	2	1	E''		22.875
2	1	0	E''	55.939	55.939	2	1	0	E''	28.833	28.847
2	1	1	E'	55.709	56.708	2	1	1	E'		28.901
2	0	1	A''_2	60.413	60.412	2	0	1	A''_2		30.908
1	1	2	E''	948.591	948.636	1	1	2	E''		752.785
1	0	2	A'_2	952.570	952.613	1	0	2	A'_2		754.810
2	2	2	E'	976.921	976.959	1	1	3	E'		756.409
1	1	3	E'	984.171	984.175	2	2	2	E'		767.202
2	1	2	E''	988.845	988.879	2	2	3	E''		770.831
2	2	3	E''	1012.534	1012.534	2	1	2	E''		773.275
2	1	3	E'	1023.714	1023.710	2	1	3	E'		776.857
2	0	3	A''_2	1027.437	1027.433	2	0	3	A''_2		778.865

^aSL = symmetry label, corresponding to the $D_{3h}(\text{M})$ molecular symmetry group. The quantum number ν_{inv} gives the number of nodes in the inversion wave function. Each ν_{inv} state of $^{14}\text{NH}_3$ has a set of “allowed” and “missing” symmetric-top energy levels (e.g., $(J, K, \nu_{\text{inv}}) = (1, 0, 1)$ of A''_1 symmetry is a missing level). Nuclear masses, in u, employed in the nuclear motion computations: $m(\text{H}) = 1.007825$, $m(\text{D}) = 2.014102$, $m(^{14}\text{N}) = 14.003074$. ^bReference 69. ^cReference 70. ^dReference 71. ^eReference 72.

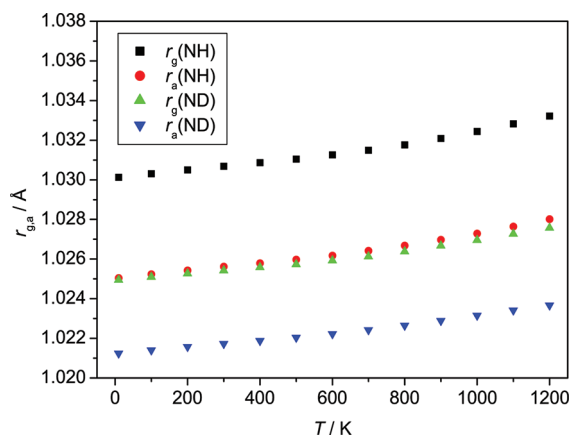


Figure 1. Temperature dependence of the “mean” ($r_{g,T}$) and “inverse” ($r_{a,T}$) bond distances of the $^{14}\text{NH}_3$ and $^{14}\text{ND}_3$ molecules, based on variational rovibrational computations and eqs 2 and 3. The linear extrapolation formula of eq 4 is used for estimating the rotational correction to the vibrational averages for $T > 300$ K. A spin-equilibrated sample is assumed (see section “On Spin Isomerism”).

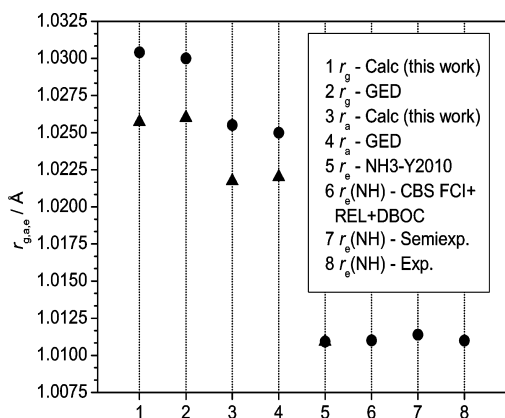


Figure 2. Graphical representation of calculated and experimental r_g , r_a , and r_e bond lengths, filled circles for NH in $^{14}\text{NH}_3$ and filled triangles for ND in $^{14}\text{ND}_3$. For explanation of the methods employed see also the footnotes to Table 3.

RESULTS AND DISCUSSION

In Table 3 estimates of equilibrium bond distances and angles of $^{14}\text{NH}_3$ are collected from the literature.^{25,30,34,38,52,54,68}

Table 4 contains $J = 1$ and 2 term values for the lowest four vibrational states of $^{14}\text{NH}_3$ and $^{14}\text{ND}_3$, computed as part of this study. For the temperature-dependent structural parameters we utilized rovibrational states of $J = 0-10$. Table 5 contains the temperature dependence of the $r_{g,T}$ and $r_{a,T}$ distances and the θ_{XNX} ($X = \text{H}$ or D) bond angle up to 1200 K, based on expectation values of the corresponding structural parameters and Boltzmann averaging. Some of the computed structural parameters are summarized in Figures 1–3.

Rotational Levels. The accuracy of the equilibrium structure given by a PES can be probed by computing rotational levels with the aid of the PES.

The small differences seen in Table 4 between the ab initio rotational level predictions and the experimental results^{69–72} clearly show the high accuracy of the underlying equilibrium structure. The slightly larger discrepancies with respect to experiment found for ND_3 are probably due to the neglect of

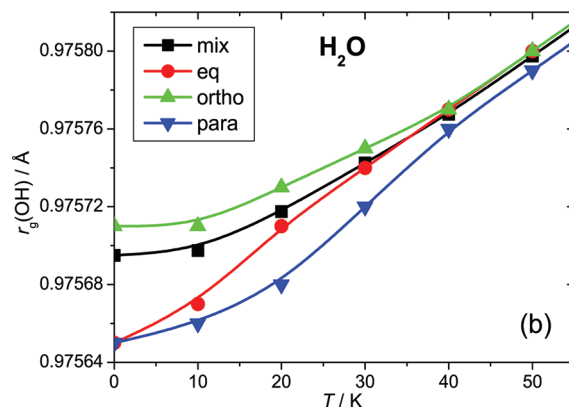
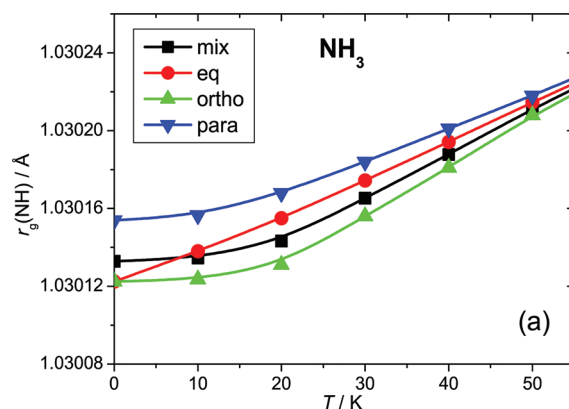


Figure 3. r_g bond lengths at low temperatures assuming different compositions of the ammonia and water samples containing two spin isomers for both cases. For $^{14}\text{NH}_3$, the ortho and para spin isomers have $I = 3/2$ and $1/2$, respectively, $o\text{-}^{14}\text{NH}_3$ is the lower-energy isomer, and the ortho to para ratio (OPR) of the “mix” sample is 2:1. For H_2^{16}O , the ortho and para spin isomers have $I = 1$ and 0, respectively, $p\text{-H}_2^{16}\text{O}$ is the lower-energy isomer, and the OPR of the “mix” sample is 3:1.

adiabatic corrections to the PES. We estimate that the equilibrium geometry parameters of ammonia, based on the NH3-Y2010 PES of ref 34, are accurate to about 2×10^{-4} Å and 0.1° .

Rovibrationally Averaged Structures. Vibrational ($J = 0$) averaging does not yield accurate effective, temperature-dependent structural parameters (Table 5). For accurate averaging the rotational corrections to the distances and angles of $^{14}\text{NH}_3$ and $^{14}\text{ND}_3$ must also be considered.

It is challenging to obtain variationally the large number of rovibrational states required to achieve convergence for the effective structural parameters at high temperatures. The way forward is to perform vibration-only ($J = 0$) computations for a large number of states up to the required energy and then employ eq 4 to estimate the rotational corrections. The σ parameters required were determined by linear fits to data points obtained by utilizing rovibrational states up to $J = 10$, allowing to converge the partition function and the effective structural parameters up to $T = 300$ K. The linear fits to data points in the temperature interval 50–300 K resulted in σ parameters for the ($\delta r_g / (\text{Å K}^{-1})$, $\delta r_a / (\text{Å K}^{-1})$, $\delta \theta_g / (\text{deg K}^{-1})$) rotational contributions of (1.92×10^{-6} , 1.95×10^{-6} , 6.34×10^{-4}) and (1.67×10^{-6} , 1.71×10^{-6} , 5.48×10^{-4}) for NH_3 and ND_3 , respectively. The correlation coefficient of the linear fitting was at least 0.998 in all cases. All the rovibrational results presented in Table 5 above $T = 300$ K were determined using this approximation.

Table 5. Temperature Dependence of Effective Structural Parameters (Distances in Å, Angles in degrees) of the $^{14}\text{NH}_3$ and $^{14}\text{ND}_3$ Molecules^a

T/K	$r_{g,T}(\text{NH})$		$r_{a,T}(\text{NH})$		$\theta_{g,T}(\text{HNNH})$	
	$J = 0$	$J \geq 0$	$J = 0$	$J \geq 0$	$J = 0$	$J \geq 0$
0	1.03012	1.03012	1.02504	1.02504	106.71	106.71
100	1.03012	1.03031	1.02504	1.02524	106.71	106.77
200	1.03012	1.03051	1.02504	1.02543	106.71	106.83
300	1.03011	1.03069	1.02503	1.02562	106.72	106.91
400	1.03010	1.03087	1.02501	1.02579	106.76	107.01
500	1.03009	1.03106	1.02500	1.02598	106.82	107.13
600	1.03011	1.03127	1.02501	1.02619	106.89	107.27
700	1.03015	1.03150	1.02505	1.02642	106.96	107.41
800	1.03023	1.03177	1.02512	1.02669	107.04	107.55
900	1.03036	1.03210	1.02522	1.02698	107.12	107.69
1000	1.03052	1.03245	1.02534	1.02730	107.19	107.82
1100	1.03071	1.03283	1.02550	1.02766	107.25	107.95
1200	1.03092	1.03324	1.02567	1.02802	107.31	108.07
T/K	$r_{g,T}(\text{ND})$		$r_{a,T}(\text{ND})$		$\theta_{g,T}(\text{DND})$	
	$J = 0$	$J \geq 0$	$J = 0$	$J \geq 0$	$J = 0$	$J \geq 0$
0	1.02493	1.02493	1.02123	1.02123	106.67	106.67
100	1.02493	1.02510	1.02123	1.02140	106.67	106.73
200	1.02493	1.02527	1.02123	1.02157	106.68	106.79
300	1.02492	1.02542	1.02122	1.02174	106.69	106.85
400	1.02491	1.02558	1.02120	1.02189	106.72	106.94
500	1.02490	1.02574	1.02119	1.02205	106.75	107.03
600	1.02492	1.02592	1.02120	1.02223	106.80	107.13
700	1.02496	1.02614	1.02123	1.02243	106.86	107.24
800	1.02504	1.02638	1.02128	1.02266	106.93	107.37
900	1.02517	1.02668	1.02135	1.02290	107.00	107.49
1000	1.02528	1.02696	1.02144	1.02316	107.07	107.61
1100	1.02543	1.02728	1.02154	1.02343	107.12	107.72
1200	1.02557	1.02759	1.02162	1.02368	107.16	107.82

^aT is the temperature in K. J is the rotational quantum number. “J = 0” refers to Boltzmann-averaged expectation values computed with vibration-only wave functions. “J ≥ 0” refers to Boltzmann-averaged expectation values computed with rovibrational wave functions up to 300 K and to vibrational averaging augmented with an approximate δr_{rot} correction for $T > 300$ K. The results may have a reduced precision of about $(1-2) \times 10^{-5}$ Å and $(2-3) \times 10^{-2}$ ° at the highest temperatures. The GED results⁵² at room temperature are: $r_g(\text{NH}) = 1.030$ Å, $r_a(\text{NH}) = 1.025$ Å, $\theta_g(\text{HNNH}) = 108.0$ °, $r_g(\text{ND}) = 1.026$ Å, $r_a(\text{ND}) = 1.022$ Å, and $\theta_g(\text{DND}) = 107.9$ °. Note the importance of the anharmonicity factors $\kappa(\text{NH})$ and $\kappa(\text{ND})$ in the GED analysis⁵² when obtaining the r_a values presented. Note also that the effective GED bond angles were based on distances corresponding to average nuclear positions and thus they do not correspond to the effective angles presented in the table.

The temperature-dependent effective structural parameters $r(^{14}\text{N}-\text{X})$ and $\theta(\text{X}-^{14}\text{N}-\text{X})$ (X = H or D) are one of the principal results of this study. They can be compared to results obtained from a GED study of Kuchitsu and co-workers.⁵² From the analysis of experimentally obtained GED radial distribution functions five types of temperature-dependent structural quantities were obtained:⁵² $r_{g,T}$, $r_{a,T}$, $\theta_{g,T}$, $l_{g,T}$, and κ . Table 5 provides the $r_{g,T}$, $r_{a,T}$, and $\theta_{g,T}$ structural parameters of the present study. The distances and angles in the “J ≥ 0” column should be compared to the experimental values obtained at about 300 K.

The computed results agree well with the GED-derived structural parameters. The GED(computed) $r_{g,T}$ and $r_{a,T}$ results for the NH distance at 300 K are $1.030 \pm 0.002(1.0307)$ and $1.025 \pm 0.002(1.0256)$ Å, respectively. The $r_{g,T}$ and $r_{a,T}$ values for the ND distance at 300 K are $1.027 \pm 0.003(1.0254)$ and $1.022 \pm 0.003(1.0217)$ Å, respectively. The temperature dependence of the NH(ND) distances and the HNH(DND) angles is significant but not large, the changes between room temperature and 1200 K are about $0.0025(0.0022)$ Å and $1.16(0.97)$ °. The distance corrections can hardly be detected by GED experiments.

The root-mean-square amplitudes of vibration at 300 K are computed to be $l_g(\text{NH}) = 0.073$ Å and $l_g(\text{ND}) = 0.062$ Å. These values can be also compared with their experimental, room-temperature counterparts,⁵² $0.073(2)$ and $0.061(2)$ Å for NH and ND, respectively. The simplified relationship⁷³ $r_g = r_a + l_g^2/r_a$ holds extremely well, as the computed $r_g - r_a$ is $0.0050(0.0037)$ Å, whereas the l_g^2/r_a values are $0.0052(0.0037)$ Å for $\text{NH}_3(\text{ND}_3)$.

On Spin Isomerism. An aspect of the present project is the investigation of the possible effects of nuclear spin on temperature-dependent, effective structural parameters of molecules.

$^{14}\text{NH}_3$ has two spin isomers, ortho (proton quartet) and para (proton doublet). These two spin isomers can be in thermal equilibrium, called “eq” in Figure 3a, or if their interconversion is not allowed, they exist as a mixture, called “mix” in Figure 3a. For $^{14}\text{NH}_3$, a natural choice for “mix” is an ortho to para ratio (OPR) of 2:1 (Table 2). Figure 3a shows the changes in the $r_g(\text{NH})$ bond length as a function of temperature for an equilibrated sample, for a mixture with an OPR of 2:1, and for the *o*- NH_3 and *p*- NH_3 spin isomers. We also note that the *o*- NH_3 to *p*- NH_3 ratio (OPR) is an important diagnostic tool

for temperature in the hands of astrophysicists and astrochemists.

According to our computations, at 0 K the $r_{g,0}(\text{N-H})$ bond lengths of *o*-NH₃ and *p*-NH₃ are 1.03012 and 1.03015 Å, respectively. Thus, the difference between the $r_{g,0}(\text{N-H})$ of the two spin isomers is 3×10^{-5} Å. The difference between the “eq” and “mix” samples is even smaller and decreases very fast, by $T = 50$ K the difference seemingly disappears. Above about $T = 50$ K the difference between the four curves diminishes below 1×10^{-5} Å, showing that in these systems nuclear spin has only a tiny effect on the effective structure. For comparison we present analogous results for the temperature dependence of $r_g(\text{O-H})$ for the two spin isomers of H₂¹⁶O in Figure 3b. In this case the natural OPR is 3:1. The results confirm clearly the trends noted for ammonia.

The data presented in Figure 3b are based on our earlier study on the structures of water isotopologues¹⁷ but were not presented there. In that study the degeneracy factors were not taken properly into account. Here we report a few corrected numbers for the $r_g(\text{OH})$ bond lengths at 100, 200, and 300 K, they are 0.97595, 0.97624, and 0.97654 Å, respectively, assuming spin equilibration. The lowest-energy expectation values for the $r_g(\text{OH})$ bond lengths of *p*-H₂O and *o*-H₂O are as follows: 0.97565 and 0.97571 Å. We also revise the σ value of ref 17 for the $r_g(\text{OH})$ bond length to 2.94×10^{-6} Å K⁻¹, which can be used to estimate the temperature dependence of the rotational corrections.

Overall, it is clear that the structural consequences of spin isomerism on the effective OH and NH bond lengths are very similar. It would be interesting to investigate further molecules in this respect.

CONCLUSIONS

On the example of the ¹⁴NH₃ and ¹⁴ND₃ molecules, we have explored the direct computational route to temperature-dependent, effective, rovibrationally averaged geometries for the class of nonlinear polyelectronic and polyatomic molecules exhibiting large-amplitude motion. This study complements our previous similar analysis on water isotopologues.¹⁷

The results obtained suggest that state-of-the-art electronic and nuclear motion computations are capable of producing effective structures for polyatomic molecules considerably more accurate than most experimental/empirical procedures can yield. The spectroscopic NH₃-Y2010 PES³⁴ employed in this study is characterized by a mass-independent (Born–Oppenheimer) equilibrium geometry of $r_e^{\text{BO}}(\text{NH}) = 1.0109$ Å and $\theta_e^{\text{BO}}(\text{HNH}) = 106.75^\circ$ and it reproduces the $J = 1$ and 2 experimental energy levels of the two investigated isotopologues of ammonia with an average accuracy of 0.005 cm⁻¹. This indicates that further empirical refinement of this PES, even if it was geared toward the lowest-lying levels, is unlikely to offer significant improvement on the equilibrium geometry parameters reported above. Uncertainties for the equilibrium bond length and bond angle of the NH₃-Y2010 PES are estimated to be 2×10^{-4} Å and 0.1°, respectively.

The most important results of this study, concerning computed r_g , r_a , r_e , θ_g , and l_g structural parameters, can be summarized as follows: (1) Vibration-only ($J = 0$) averaging does not yield correct effective bond length increments even over a rather large temperature range. (2) Distance corrections due to rotations are substantial even at relatively low temperatures. For temperatures higher than about 50 K, rotational corrections to the distances turn out to be linearly dependent upon the temperature. This observation allows an extrapolation to higher

temperatures, an important result when one wants to treat larger systems. (3) The effect of nuclear spin on geometry parameters is small but non-negligible at low temperatures, below about 50 K, and at the level of precision that can be obtained for smaller molecules. The difference between the $r_g(\text{N-H})$ bond lengths of *o*-NH₃ and *p*-NH₃ is 3×10^{-5} Å at 0 K. (4) GENIUSH and any similar nuclear-motion algorithms employing internal coordinates in the Hamiltonian can handle perfectly well the effect of large-amplitude inversion motion on structural parameters.

AUTHOR INFORMATION

Corresponding Author

*E-mail: csaszar@chem.elte.hu.

Notes

The authors declare no competing financial interest.

ACKNOWLEDGMENTS

This work was supported by the Hungarian Scientific Research Fund (OTKA K72885 and NK83583). The European Union and the European Social Fund have provided financial support to this project under Grant No. TÁMOP-4.2.1/B-09/1/KMR-2010-0003. The authors thank Dr. Sergei Yurchenko for providing the PES of ref 34.

REFERENCES

- (1) Born, M.; Oppenheimer, J. R. *Ann. Phys.* **1927**, *84*, 457.
- (2) Born, M.; Huang, K. *Dynamical Theory of Crystal Lattices*; Oxford University Press: New York, 1954.
- (3) Bunker, P. R.; Jensen, P. *Computational Molecular Spectroscopy*; Wiley: New York, 2000; pp 3–11.
- (4) Mezey, P. G. *Potential Energy Hypersurfaces*; Elsevier: Amsterdam, 1979.
- (5) Murrell, J. N.; Carter, S.; Farantos, S. C.; Huxley, P.; Varandas, A. J. C. *Molecular Potential Energy Surfaces*; Wiley: New York, 1984.
- (6) Császár, A. G.; Allen, W. D.; Yamaguchi, Y.; Schaefer, H. F. Ab initio determination of accurate ground electronic state potential energy hypersurfaces for small molecules. In *Computational Molecular Spectroscopy*; Jensen, P., Bunker, P. R., Ed.; John Wiley & Sons: London, 2000; pp 15–68.
- (7) Demaison, J.; Boggs, J. E.; Császár, A. G. *Equilibrium Molecular Structures*; CRC Press: Boca Raton, FL, 2011.
- (8) Watson, J. K. G. *J. Mol. Spectrosc.* **2004**, *223*, 39.
- (9) Demaison, J.; Włodarczyk, G.; Rudolph, H. D. *Advances in Molecular Structure Research*; JAI Press: Greenwich, CT, 1997; Vol. 3, pp 1–51.
- (10) Margules, L.; Demaison, J.; Boggs, J. E. *J. Phys. Chem. A* **1999**, *103*, 7632.
- (11) Demaison, J.; Breidung, J.; Thiel, W.; Papoušek, D. *Struct. Chem.* **1999**, *10*, 129.
- (12) Kuchitsu, K.; Morino, Y. *Bull. Chem. Soc. Jpn.* **1965**, *38*, 805.
- (13) Kuchitsu, K.; Morino, Y. In *Molecular Structure and Vibrations*; Cyvin, S. J., Ed.; Elsevier: Amsterdam, 1972; p 183.
- (14) Kuchitsu, K. In *Accurate Molecular Structures: Their Determination and Importance*; Domenicano, A., Hargittai, I., Eds.; Oxford University Press: Oxford, U.K., 1992; pp 14–46.
- (15) Sutcliffe, B. T. *Lect. Notes Chem.* **2000**, *74*, 3.
- (16) Sutcliffe, B. T. *Int. J. Quantum Chem.* **2002**, *90*, 66.
- (17) Czako, G.; Mátyus, E.; Császár, A. G. *J. Phys. Chem. A* **2009**, *113*, 11665.
- (18) Demaison, J.; Császár, A. G.; Kleiner, I.; Møllendal, H. *J. Phys. Chem. A* **2007**, *111*, 2574.
- (19) Kuchitsu, K.; Oyanagi, K. *Faraday Discuss.* **1977**, *62*, 20.
- (20) Császár, A. G.; Fábri, C.; Szidarovszky, T.; Mátyus, E.; Furtenbacher, T.; Czako, G. *Phys. Chem. Chem. Phys.* **2012**, *14*, 1085.

- (21) Cheung, A. C.; Rank, D. M.; Townes, C. H.; Thornton, D. D.; Welch, W. J. *Nature* **1969**, *221*, 626.
- (22) Špirko, V.; Kraemer, W. P. *J. Mol. Spectrosc.* **1989**, *133*, 331.
- (23) Martin, J. M. L.; Lee, T. J.; Taylor, P. R. *J. Chem. Phys.* **1992**, *97*, 8361.
- (24) Lin, H.; Thiel, W.; Yurchenko, S. N.; Carvajal, M.; Jensen, P. *J. Chem. Phys.* **2002**, *117*, 11265.
- (25) Rajamäki, T.; Miani, A.; Halonen, L. *J. Chem. Phys.* **2003**, *118*, 10929.
- (26) Leonard, C.; Carter, S.; Handy, N. C. *Chem. Phys. Lett.* **2003**, *370*, 360.
- (27) Lauvergnat, D.; Nauts, A. *Chem. Phys.* **2004**, *305*, 105.
- (28) Marquardt, R.; Sagui, K.; Klopper, W.; Quack, M. *J. Phys. Chem. B* **2005**, *109*, 8439.
- (29) Yurchenko, S. N.; Zheng, J.; Lin, H.; Jensen, P.; Thiel, W. *J. Chem. Phys.* **2005**, *123*, 134308.
- (30) Huang, X.; Schwenke, D. W.; Lee, T. J. *J. Chem. Phys.* **2008**, *129*, 214304.
- (31) Yurchenko, S. N.; Barber, R. J.; Yachmenev, A.; Thiel, W.; Jensen, P.; Tennyson, J. *J. Phys. Chem. A* **2009**, *113*, 11845.
- (32) Li, Y. Q.; Varandas, A. J. C. *J. Phys. Chem. A* **2010**, *114*, 6669.
- (33) Huang, X.; Schwenke, D. W.; Lee, T. J. *J. Chem. Phys.* **2011**, *134*, 044320.
- (34) Yurchenko, S. N.; Barber, R. J.; Tennyson, J.; Thiel, W.; Jensen, P. *J. Mol. Spectrosc.* **2011**, *268*, 123.
- (35) Kauppi, E.; Halonen, L. *J. Chem. Phys.* **1995**, *103*, 6861.
- (36) Császár, A. G.; Allen, W. D.; Schaefer, H. F., III. *J. Chem. Phys.* **1998**, *108*, 9751.
- (37) Klopper, W.; Samson, C. C. M.; Tarczay, G.; Császár, A. G. *J. Comput. Chem.* **2001**, *22*, 1306.
- (38) Rajamäki, T.; Kállay, M.; Noga, T.; Valiron, P.; Halonen, L. *Mol. Phys.* **2004**, *102*, 2297.
- (39) Puzzarini, C. *Theor. Chem. Acc.* **2008**, *121*, 1.
- (40) Gordon, J. P.; Zeiger, H. J.; Townes, C. H. *Phys. Rev.* **1954**, *95*, 282.
- (41) Müller, H.; Kutzelnigg, W.; Noga, J. *Mol. Phys.* **1997**, *92*, 535.
- (42) Mátyus, E.; Czako, G.; Sutcliffe, B.; Császár, A. G. *J. Chem. Phys.* **2007**, *127*, 084102.
- (43) Yurchenko, S. N.; Thiel, W.; Jensen, P. *J. Mol. Spectrosc.* **2007**, *245*, 126.
- (44) Mátyus, E.; Šimunek, J.; Császár, A. G. *J. Chem. Phys.* **2009**, *131*, 074106.
- (45) Mátyus, E.; Czako, G.; Császár, A. G. *J. Chem. Phys.* **2009**, *130*, 134112.
- (46) Fábri, C.; Mátyus, E.; Császár, A. G. *J. Chem. Phys.* **2011**, *134*, 074105.
- (47) Benedict, W. S.; Plyler, E. K. *Can. J. Phys.* **1957**, *35*, 1235.
- (48) Morino, Y.; Kuchitsu, K.; Yamamoto, S. *Spectrochim. Acta* **1968**, *A24*, 335.
- (49) Bunker, P. R.; Kraemer, W. P.; Špirko, V. *Can. J. Phys.* **1984**, *62*, 1801.
- (50) Almenningen, A.; Bastiansen, O. *Acta Chem. Scand.* **1955**, *9*, 815.
- (51) Bastiansen, O.; Beagley, B. *Acta Chem. Scand.* **1964**, *18*, 2077.
- (52) Kuchitsu, K.; Guillory, J. P.; Bartell, L. S. *J. Chem. Phys.* **1963**, *49*, 2488.
- (53) Tvard, C.; Roualt, M.; Roux, M.; Cornille, M. *J. Chem. Phys.* **1963**, *39*, 2390.
- (54) Demaison, J.; Margulés, L.; Boggs, J. E. *Chem. Phys.* **2000**, *260*, 65.
- (55) Bunker, P. R.; Jensen, P. *Molecular Symmetry and Spectroscopy*; NRC Research: Ottawa, 1998.
- (56) Császár, A. G.; Tarczay, G.; Leininger, M. L.; Polyansky, O. L.; Tennyson, J.; Allen, W. D. In *Spectroscopy from Space*; Demaison, J., Sarka, K., Cohen, E. A., Eds.; Kluwer: Dordrecht, 2001; pp 317–339.
- (57) Douglas, M.; Kroll, N. M. *Ann. Phys.* **1974**, *82*, 89.
- (58) Tarczay, G.; Császár, A. G.; Klopper, W.; Quiney, H. M. *Mol. Phys.* **2001**, *99*, 1769.
- (59) Wolf, A.; Reiher, M.; Hess, B. A. *J. Chem. Phys.* **2004**, *120*, 8624.
- (60) Handy, N. C.; Yamaguchi, Y.; Schaefer, H. F. *J. Chem. Phys.* **1986**, *84*, 4481.
- (61) Harris, D. O.; Engerholm, G. G.; Gwinn, W. D. *J. Chem. Phys.* **1965**, *43*, 1515.
- (62) Dickinson, A. S.; Certain, P. R. *J. Chem. Phys.* **1968**, *49*, 4209.
- (63) Lanczos, C. *J. Res. Natl. Bur. Stand.* **1950**, *45*, 255.
- (64) Nielsen, H. H. *Rev. Mod. Phys.* **1951**, *23*, 90.
- (65) Mills, I. M. In *Molecular Spectroscopy: Modern Research*; Rao, K. N.; Mathews, C. W., Eds.; Academic Press: New York, 1972.
- (66) Iwasaki, M.; Hedberg, K. *J. Chem. Phys.* **1962**, *36*, 2961.
- (67) Toyama, M.; Oka, T.; Morino, Y. *J. Mol. Spectrosc.* **1964**, *13*, 193.
- (68) Pawlowski, F.; Jørgensen, P.; Olsen, J.; Hegelund, F.; Helgaker, T.; Gauss, J.; Bak, K. L.; Stanton, J. F. *J. Chem. Phys.* **2002**, *116*, 6482.
- (69) Urban, S.; D’Cunha, R.; Rao, N.; Papoušek, D. *Can. J. Phys.* **1984**, *62*, 1775.
- (70) Chen, P.; Pearson, J. C.; Pickett, H. M.; Matsuura, S.; Blake, G. A. *J. Mol. Spectrosc.* **2006**, *236*, 116.
- (71) Fusina, L.; Murzin, S. N. *J. Mol. Spectrosc.* **1994**, *167*, 464.
- (72) Coudert, L. H.; Roueff, E. *Astron. Astrophys.* **2006**, *449*, 855.
- (73) Bartell, L. S. *J. Chem. Phys.* **1955**, *23*, 1219.